Cohesive Zone Models in the Characterisation of Toughness

J.G. Williams, H. Hadavinia and A.J. Kinloch

Department of Mechanical Engineering, Imperial College London, Exhibition Road, London, SW7 2AZ, UK.

Abstract

Cohesive zone models (CZMs) may be used in conjunction with finite element (FE) analysis to characterise the toughness of composites delamination and adhesive joints. The method uses two parameters, the fracture energy G_c and the cohesive stress $\bar{\sigma}$ and varying these parameters enables the analysis to describe a wide range of both initiation and steady-state propagation behaviour. The usual scheme is to determine G_c and $\bar{\sigma}$ by an inverse method by fitting experimental results, and examples will be given of values obtained in delamination and peeling tests. The significance of the values will be discussed and particularly the relationship of $\bar{\sigma}$ to a constrained yield stress. Other interpretations of the behaviour such as stiffness control will also be considered.

1. Introduction

The use of cohesive zone models, or traction-separation laws, to define fracture processes is now widely employed. The fracture process, as the crack propagates, is modelled in terms of a local stress-displacement relationship. The local work done is the area under the curve and is the fracture toughness G_c and the final displacement is that at the crack tip and is equivalent to the crack opening displacement v_0. The process may also be defined via the maximum, or cohesive stress, $\bar{\sigma}$, in the zone. The shape of the curve is also a possible variable, including parameters such as the initial stiffness and shape of the decreasing part of the curve. Fig. 1. shows some possible shapes ranging from the very simple Dugdale or constant stress (a), through various triangular types (b)-(d), to a combination; the trapezoidal (e), and the cubic (f). The various parameters are listed in the following Table in which, in addition to the values of $\bar{\sigma}$ and v_0, we have λ to define the shape and the initial (rising) stiffness S.

Model	(a)	(b)	(c)	(d)	(e)	(f)
$G_c / \bar{\sigma} v_0$	1	1/2	1/2	1/2	$(1+\lambda_2-\lambda_1)/2$	9/16
$S v_0 / \bar{\sigma}$	∞	1	∞	$1/\lambda$	$1/\lambda_1$	27/4
$S_1 v_0 / \bar{\sigma}$	-∞	-∞	-1	$-1/(1-\lambda)$	$-1/(1-\lambda_2)$	0

The shape of the curve does not greatly influence the form of the G_c determination and even the most flexible form, (e), gives the range $1/2 < G_c / \bar{\sigma} v_0 < 1$. Thus, if $\bar{\sigma}$ and G_c are fixed, the relationship to v_0 is similar in all the forms. The two stiffness parameters are however, subject to wide variation dependent upon the shape. The trapezoidal form, (e), is widely used because it is flexible and the cubic, (f), because it is convenient in the FE codes.

The fundamental question to be addressed is how do we decide upon, or determine, the parameters in such models? It is generally accepted that G_c is a basic parameters of fracture, though with plastic deformation its value may be stress-state dependent. For high constraint (plane strain) it is assumed to have a minimum value and that the plasticity is confined to a small local region at the crack tip. This implies a high $\bar{\sigma}$ in the model and in such circumstances fracture is governed by a single parameter, G_c, and is independent of $\bar{\sigma}$. This is linear elastic fracture mechanics (LEFM). When $\bar{\sigma}$ is not large then the length scale becomes important and much more complex behaviour occurs. This may be illustrated by the simple model of a cantilever with a Dugdale zone as shown in Fig. 2.

2. The Cantilever Model

The geometry of this model is shown in Fig. 2 and the elastic solution for the energy release is:

$$G = \frac{6(Pa)^2}{Eb^2h^3}$$

when a constant stress zone (Fig 1a) is present the length ℓ is given by:

$$\ell^2 = \left(\frac{2P}{\bar{\sigma} b}\right)(a+\ell)$$

and: $$G = \frac{6P^2 a}{Eb^2 a^3}(a+\ell)(a+\ell/3)$$

and hence when $\bar{\sigma} \to \infty$, $\ell \to 0$ and G tends to the elastic solution. For a crack propagating at $G = G_c$ constant, these two relationships give:

$$\left(\frac{\ell}{h}\right)^4 \left(\frac{a+\ell/3}{a+\ell}\right) = \frac{2}{3}\frac{EG_c}{h\bar{\sigma}^2} = \left(\frac{\bar{\ell}}{h}\right)^4$$

Thus ℓ is not constant during propagation but varies from $3^{1/4}\bar{\ell} = 1.3\ell$ to $\bar{\ell}$ as a varies from zero to $a >> \bar{\ell}$, i.e. it changes only slightly during propagation and a reasonable approximation is $\ell = \bar{\ell}$. The end deflection is given by:

$$\delta = \frac{4}{E}\left(\frac{P}{bh^3}\right)(a+\ell)(a+\ell/2)^2$$

so that the compliance, δ / P, on initial loading is dependent on ℓ and hence $\bar{\sigma}$. The value of ℓ is also dependent on P and hence there will be nonlinearity for large ℓ. For constant G_c propagation, we have:

$$\left(\frac{P}{bhE}\right) = \left(\frac{2}{27}\right)^{1/4} \left(\frac{G_c}{Eh}\right)^{3/4} \left(\frac{h}{\delta}\right)^{1/2}$$

for $\bar{\ell} << a$, i.e. a load-displacement relationship which is independent of $\bar{\sigma}$. This type of test has been explored numerically using FE and the cubic form of traction-separation law [1]. Fig. 3 from [1] shows the load-displacement data for a fixed G_c (257 J/m^2) and various values of $\bar{\sigma}$ compared with experimental data for a carbon fibre polymer composite (CFRP) in a double cantilever beam (DCB) test. The decreasing stiffness with decreasing $\bar{\sigma}$ is apparent as well as the onset of nonlinearity. The propagation data is sensibly independent of $\bar{\sigma}$ as expected. Interestingly, the fit to the initial stiffness implies high (>30 MPa) values of $\bar{\sigma}$, but it is not possible to define a value with any certainty.

The DCB test also provides an example of how a different model may give an equally good fit to the observations. For the composites case an elastic analysis of the region beyond the crack tip provides a linear stiffness version of the traction law, see Fig. 1b, but in which S may be computed [2]. This gives an explicit expansion for $\bar{\ell}$ [2]:

$$\left(\frac{\bar{\ell}}{h}\right)^4 = \left[0.1\frac{E_1}{\mu} - 0.06 + 0.24\sqrt{\frac{E_1}{E_2}}\right]^2$$

where E_1, E_2 and μ are the axial, transverse and shear modulii, respectively. For a typical composite, as used here, $\bar{\ell}/h \approx 2.5$ and the same expression for the maximum stress applies although now $\bar{\sigma}$ only acts at $x = 0$. This gives:

$$\bar{\sigma}^2 = \frac{2}{3}\left(\frac{h}{\ell}\right)^4 \frac{EG_c}{h} = 0.017\left(\frac{EG_c}{h}\right)$$

For the parameters used here, $E_1 = 140$ GPa, $G_c = 257$ J/m^2, $h = 1.5$ mm we have $\bar{\sigma} = 20$ MPa, which fits the data well.

This CFRP DCB case also illustrates some general points. Firstly, this is an elastic system with local damage. The initial response is essentially linear indicating high $\bar{\sigma}$ values. The FE data fits suggest a high $\bar{\sigma}$ but the propagation results, which are steady state, serve only to fix G_c. Without knowing $\bar{\sigma}$, recourse is made to a stiffness analysis which works well and defines $\bar{\sigma}$. Here $\bar{\sigma}$ is close to a local failure stress but could not be defined prior to the testing whilst the stiffness, of course, can. More refined studies show that measured $\bar{\ell}$ values may be compared to the elastic cases and define $\bar{\sigma}$ and the damage more precisely [3].

3. Peel Testing

The peeling of flexible laminates, as shown in Fig. 4, provides an example of a fracture process accompanied by extensive plastic deformation. In this case the free arm often undergoes plastic bending and unbending as the debonding proceeds and, for a 90° peel, as shown here, the total energy dissipated per unit area G is given by P/b. This is the sum of the true adhesive energy G_c and the plastic dissipation, G_d. The latter can be computed [1] to correct G and G_d is often a significant proportion of G (up to 90%). G_d is a strong function of the root rotation θ_0 and this may be computed using a CZM, as shown; using either a FE [1] or an analytical model. As in the previous example we may define $\bar{\sigma}$, or use a stiffness based analytical solution which can also determine $\bar{\sigma}$. Examples of such analyses is shown in Fig. 5, as G_c versus $\bar{\sigma}$. The solid line represents the linear-shaped zone analytical model, see Fig. 1b, which is given by:

$$\bar{\sigma} = 2.1\frac{X^{0.5}(1-X)^{1.64}}{(X-0.091)^2} \quad \text{(MPa)} \qquad X = G_c/G$$

for power law work hardening with n=0.22, [1]. In an experiment G was 5400 J/m^2 and a separate LEFM test gave $G_c = 1080 \pm 100$ J/m^2, which is also shown. The stiffness controlled solution is a particular point on that line and is at 890 J/m^2 and 120 MPa. The G_c value is somewhat lower than that from the LEFM test and $\bar{\sigma}$ is about 2.1 times the adhesive yield stress which is 50 MPa, and this gives of course a constraint factor of 2.1.

Three cases were run in FE, i.e. $\bar{\sigma} = 30$, 40 and 50 MPa, using the cubic-shaped CZM and the values were also shown in Fig. 5. The G_c values are about 7% less than the analytical case. The ‘corrected’ values shown in Fig. 5 were calculated to give agreement with the analytical results and were obtained when the stresses were increased by 20%, and such an effect is probably due to the shape of the traction-curve. For example, for given values of G_c and v_0, the ratio of the resulting values of $\bar{\sigma}$ for the linear (Fig1b) compared with the cubic (Fig 1f) shaped CZM would be 18/16=1.13. It should be noted that no results could be obtained with FE for $\bar{\sigma} > 50$ MPa, since the programme crashed for all larger values. Certainly it seems that in this case $\bar{\sigma}$ is limited to the unconstrained yield stress and that the assumption of stiffness control leads to too high a constraint factor.

4. Conclusion

The LEFM delamination tests illustrate the difficulty of defining $\bar{\sigma}$ even for elastically dominated systems. The initial stiffness of the loading curve defines it best, but only to the extent of saying that it must be above some value. The propagation phase is dependent solely on the value of G_c. The local elastic model provides a good fit to the data and can be predetermined. For the peel test the stiffness model gave a rather high value of $\bar{\sigma}$ and limiting it to about the adhesive yield stress gives the best fit to G_c. This indicates a lack of constraint in the adhesive layer during fracture. These two examples indicate the range of behaviour it is possible to model and the uncertainty in defining $\bar{\sigma}$.

References

[1] Blackman, B.R.K., Hadavinia, H., Kinloch, A.J. and Williams, J.G., '*The use of cohesive zone model to study the fracture of fibre composites and adhesively-bonded joints*', Int. Journal of Fracture, Vol. 119(1): 25–46, 2003.

[2] Williams, J.G. and Hadavinia, H., '*Elastic and elastic-plastic correction factors for DCB specimens*', 14th European Conference on Fracture – ECF 14 Fracture Mechanics Beyond 2000, Cracow, Poland, EMAS Publishing, Vol. 3: 573-592, 2002.

[3] Brunner, A.J., B.R.K. Blackman, and J.G. Williams. '*Deducing bridging stresses and damage from G_{IC} tests on fibre composites*'. In Fracture of Polymers, Composites and Adhesives II. Les Diablerets, Switzerland: ESIS Publication 32, pp 479-490, Elsevier Science Ltd. 2002.

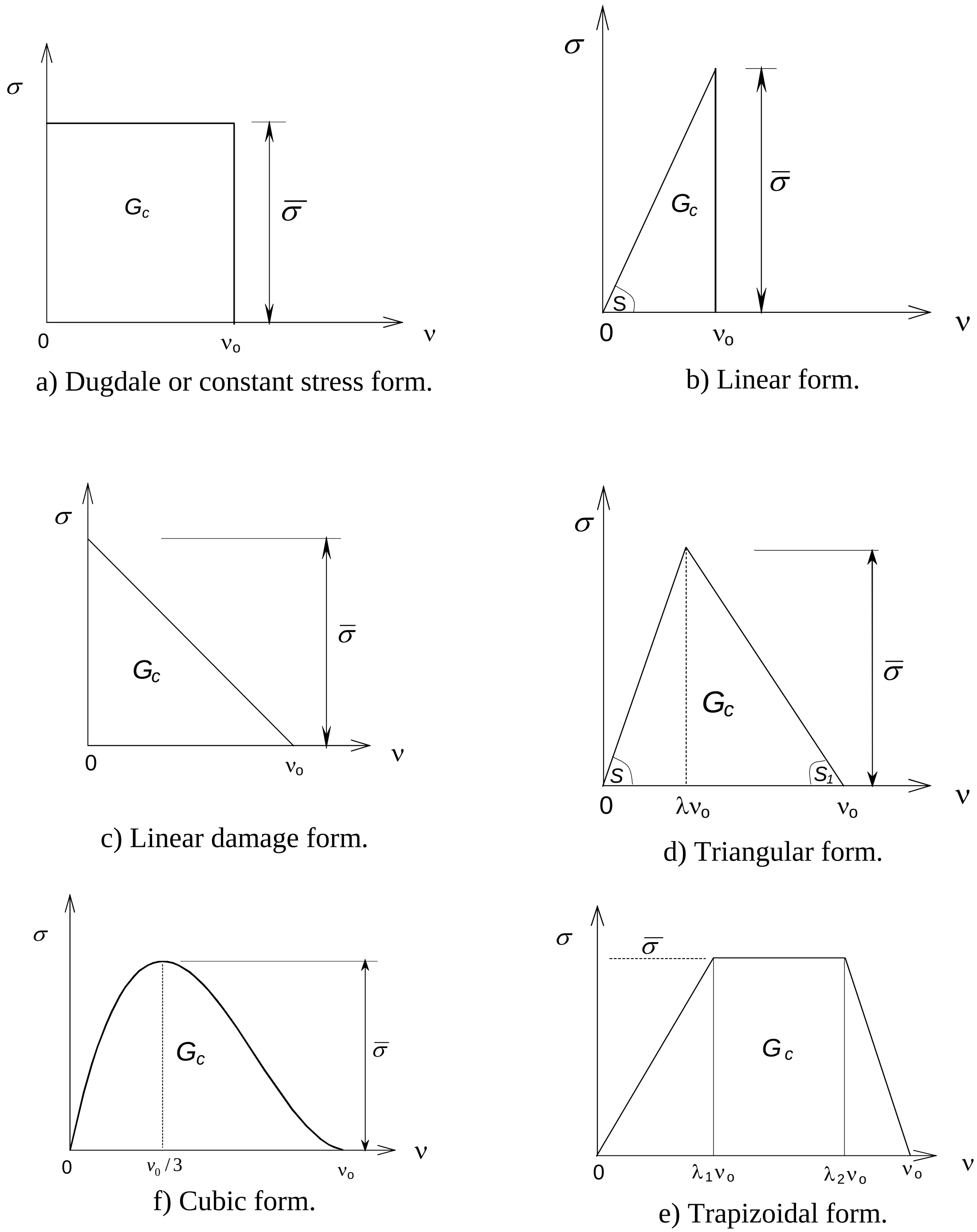

a) Dugdale or constant stress form.

b) Linear form.

c) Linear damage form.

d) Triangular form.

f) Cubic form.

e) Trapizoidal form.

FIG. 1. Forms of traction separation laws.

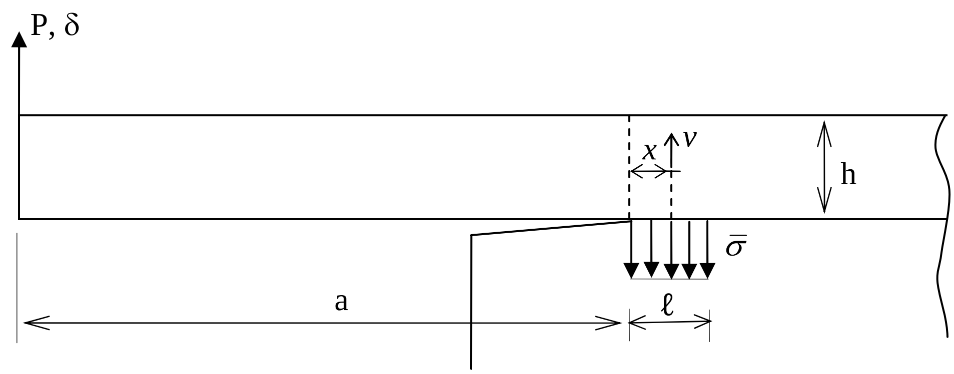

FIG. 2. The cantilever model with a constant stress zone.

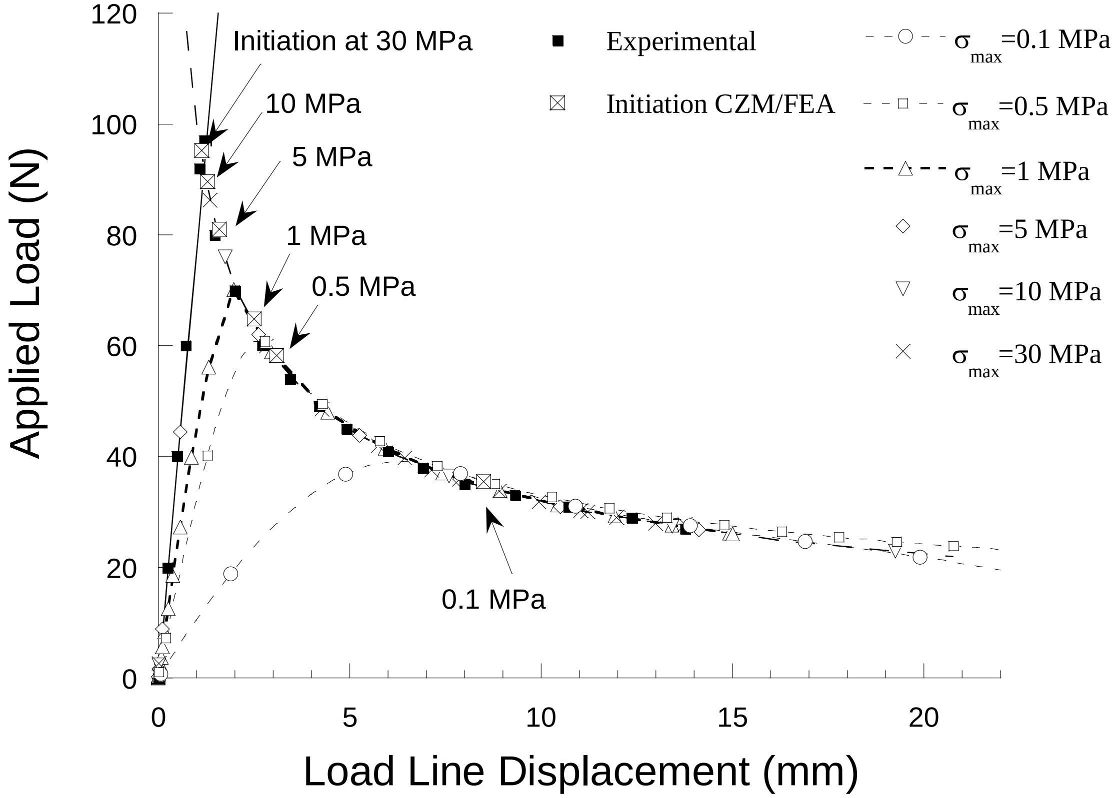

FIG. 3. Load displacement data for a CFRP, DCB test.

NOTE: $\bar{\sigma} = \sigma_{max}$

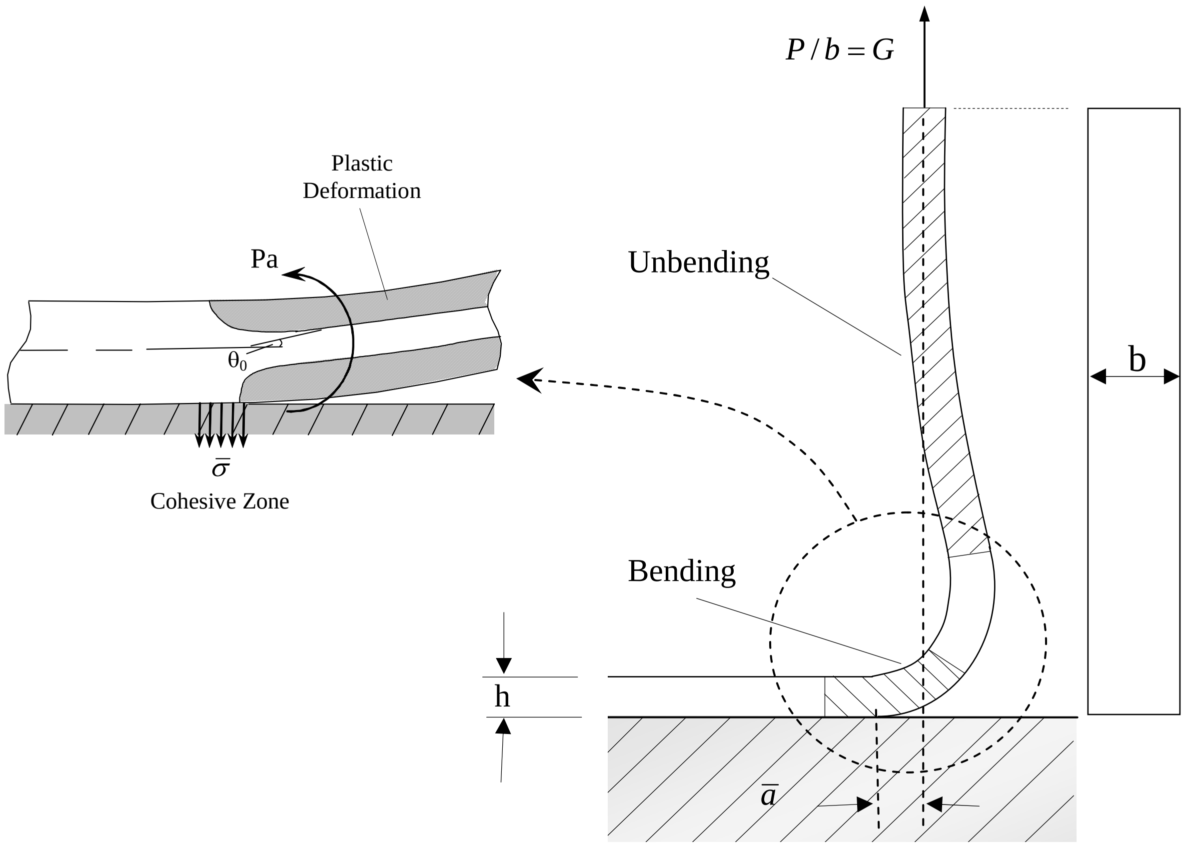

FIG. 4. The peeling of a flexible laminate.

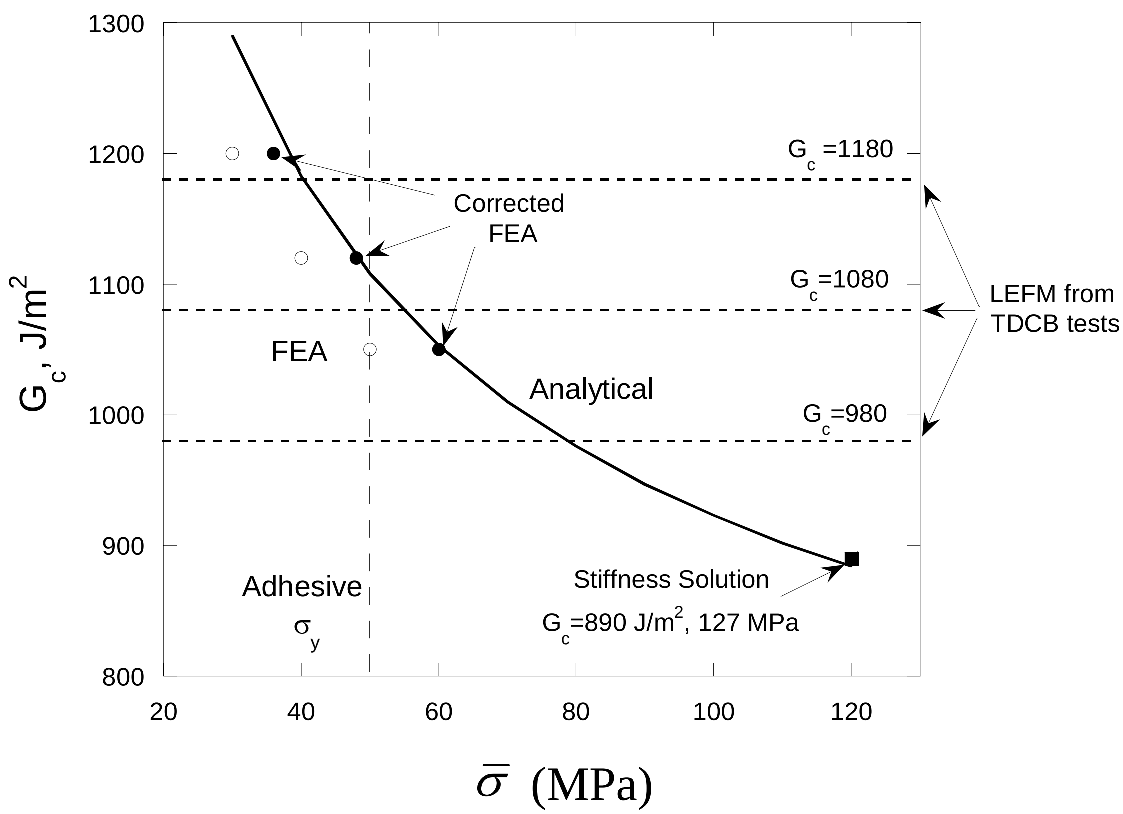

FIG. 5. G_c as a function of $\bar{\sigma}$ for a peel test.